

# 12 nm-Gate-Length Ultrathin-Body InGaAs/InAs MOSFETs with $8.3 \cdot 10^5 I_{ON}/I_{OFF}$

Cheng-Ying Huang<sup>1</sup>, Prateek Choudhary<sup>1</sup>, Sanghoon Lee<sup>1</sup>, Stephan Kraemer<sup>2</sup>, Varistha Chobpattana<sup>2</sup>, Brain Thibeault<sup>1</sup>, William Mitchell<sup>1</sup>, Susanne Stemmer<sup>2</sup>, Arthur Gossard<sup>1,2</sup>, and Mark Rodwell<sup>1</sup>

<sup>1</sup>ECE Department, <sup>2</sup>Materials Department, University of California, Santa Barbara, CA 93106 USA

Email: [cyhuang@ece.ucsb.edu](mailto:cyhuang@ece.ucsb.edu), TEL: 805-886-2630

**Introduction:** III-V InGaAs/InAs MOSFETs can provide high on-state current at lower  $V_{DD}$ , and are being considered as promising candidates to replace Si channels at future 7 or 5 nm technology nodes. At the 5 nm node, the International Technology Roadmap for Semiconductors (ITRS) targets 12 nm physical gate length [1]. At such small dimensions, few III-V MOSFETs have been reported, and the observed off-state leakage currents have been high [2-8]. High off-state leakage current arising from band-to-band tunneling (BTBT) near the drain end of channel makes it difficult to scale III-V MOSFETs to sub-10-nm generations. Previously we reported a FET using a 2.5 nm thick InAs channel to reduce  $I_{off}$  to 10 nA/ $\mu\text{m}$  for 25 nm  $L_g$ , simultaneously achieving record  $I_{on}$  (500  $\mu\text{A}/\mu\text{m}$  at 100 nA/ $\mu\text{m}$   $I_{off}$  and  $V_{DD}=0.5$  V) [9]. To further reduce BTBT leakage current, we developed InGaAs-channel MOSFETs with 4.5 nm thick channels and graded-doping recessed InP source/drain spacer layers; these showed a minimum 60 pA/ $\mu\text{m}$   $I_{off}$  at 30 nm  $L_g$  [10]. Here, we further reduce the physical gate length, and report 12 nm- $L_g$  FETs with 1.5/1 nm InGaAs/InAs composite channels, and recessed doping-graded InP source/drain spacers. The FETs demonstrate high  $\sim 1.8$  mS/ $\mu\text{m}$  transconductance ( $g_m$ ), low  $\sim 107$  mV/dec. subthreshold swing ( $SS$ ), and low  $\sim 1.3$  nA/ $\mu\text{m}$  minimum  $I_{off}$  at  $V_{DS}=0.5$  V. For the first time, III-V InGaAs/InAs MOSFETs at 12 nm gate length were demonstrated with well-balanced on-off DC performance. The maximum  $I_{on}/I_{off}$  at  $V_{DS}=0.5$  V is  $8.3 \times 10^5$ , confirming that III-V MOSFETs are scalable to sub-10-nm technology nodes.

**Device Fabrication:** Fig. 1 shows the device structure; [9,10] give the detailed process flow. The channel consists of a 1 nm InAs bottom channel and a 1.5 nm  $\text{In}_{0.53}\text{Ga}_{0.47}\text{As}$  top channel. The devices have 12 to 1000 nm physical gate lengths (defined by the edges of regrown layers as shown in Fig. 2a). The InGaAs layer in the source/drain (S/D) region was partially removed by a digital etch, leaving  $\sim 0.5$  nm InGaAs and 1 nm InAs to prevent the oxidation of the InAlAs barriers and ensure high crystalline quality MOCVD regrowth. The S/D layers grown by MOCVD have an un-doped InP spacer, a linearly doping-graded InP spacer, a Si-doped InP ( $\sim 5 \times 10^{19} \text{ cm}^{-3}$ ) layer and a Si-doped ( $4.0 \times 10^{19} \text{ cm}^{-3}$ )  $\text{In}_{0.53}\text{Ga}_{0.47}\text{As}$  contact layer. The FETs have a  $\sim 3.4$  nm  $\text{ZrO}_2$  gate dielectric, including the AlON interfacial layer formed by the ALD cyclic TMA/nitrogen plasma pre-treatment. Ni/Au gate and Ti/Pd/Au S/D metal contacts were defined using liftoff. Fig. 2b shows the cross-sectional TEM images of a 12 nm- $L_g$  device.

**Results:** Fig. 3 shows transfer characteristics of a 12 nm- $L_g$  FET, achieving 1.8 mS/ $\mu\text{m}$  peak  $g_m$  at  $V_{DS}=0.5$  V. The subthreshold swing, Fig. 4, is 98.6 mV/dec. at  $V_{DS}=0.1$  V and 107.5 mV/dec. at  $V_{DS}=0.5$  V. The minimum leakage current is as low as 1.3 nA/ $\mu\text{m}$  at  $V_{DS}=0.5$  V, where  $I_{off}$  is limited by BTBT. This leakage current is sufficiently low to meet the requirement of high performance (HP, 100 nA/ $\mu\text{m}$ ) logic applications, and close to the specification of standard performance (SP, 1 nA/ $\mu\text{m}$ ) applications. Fig. 5 shows the output characteristics of a 12 nm- $L_g$  FET. The maximum  $I_D$  exceeds 1.25 mA/ $\mu\text{m}$  at  $V_{GS}=1.2$  V and  $V_{DS}=0.7$  V, and the on-resistance ( $R_{on}$ ) at  $V_{GS}=1$  V is 302  $\Omega \cdot \mu\text{m}$ . The  $I_D$  at  $V_{GS}=1.2$  V and  $V_{DS}=0.5$  V is 1.1 mA/ $\mu\text{m}$ , showing maximum  $I_{on}/I_{off} \sim 8.3 \times 10^5$ . Examining (Fig. 6)  $g_m$  as a function of  $L_g$ , the present InGaAs/InAs channel devices show  $g_m$  slightly superior to our previously-reported devices using InP spacers and InGaAs channels [10] but lower  $g_m$  than devices using InGaAs spacers and InAs channels [9]. On-resistance, Fig. 7,  $\sim 262 \Omega \cdot \mu\text{m}$  when extrapolated to zero  $L_g$ , is also consistent with earlier results using similar InP spacers [10].

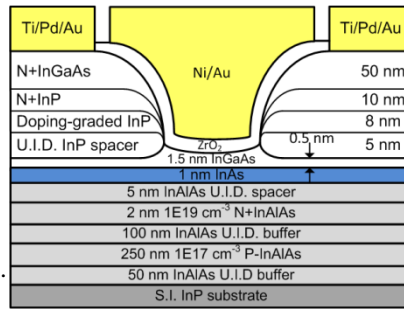
Fig. 8 shows  $SS$  vs.  $L_g$  and Fig. 9 shows DIBL vs.  $L_g$ . As gate length decreases,  $SS$  and DIBL increase due to deteriorating electrostatics. Further thinning the channel would reduce such short-channel effects, but unfortunately we have found that InGaAs channels thinner than  $\sim 3.5$  nm show poor  $g_m$ . InAs channels, in contrast, though showing high  $g_m$  even when 2.5 nm thick, show high BTBT leakage [9]. A tri-gate structure would improve electrostatics, allowing use of thicker channels and thinner source/drain spacers. Because only a thin InP high-field drain spacer layer would be required to suppress BTBT, on-state performance ( $g_m$ ) would be improved [10].

Fig. 10 shows minimum  $I_{off}$  vs.  $L_g$ . The FETs reported here, having a 1.5/1 nm InGaAs/InAs composite channel and recessed InP spacers, show lower leakage current than FETs using 2.5 nm InAs channels and InGaAs S/D spacers [9], but larger leakage than FETs using 4.5 nm InGaAs channels and recessed InP spacers [10]. A clear tradeoff between  $I_{on}$  and  $I_{off}$  is observed in Figs. 6, 10 and 11. Fig. 11 benchmarks  $I_{on}$  as a function of  $L_g$  at  $I_{off}=100$  nA/ $\mu\text{m}$  and  $V_{DS}=V_{GS}-V_{TH}=0.5$  V. The FETs reported here show  $I_{on} \sim 311 \mu\text{A}/\mu\text{m}$  at  $L_g=42$  nm, similar to [10].

**Conclusion:** We report III-V MOSFETs with 12 nm physical gate length, ultrathin 1.5/1 nm InGaAs/InAs composite channels, and recessed doping-graded InP S/D vertical spacers. The FETs demonstrate  $g_m \sim 1.8$  mS/ $\mu\text{m}$  transconductance,  $SS \sim 107$  mV/dec., minimum  $I_{off} \sim 1.3$  nA/ $\mu\text{m}$  at  $V_{DS}=0.5$  V, and well-balanced on-off DC performance with maximum  $I_{on}/I_{off} \sim 8.3 \times 10^5$ . Band-to-band tunneling leakage current is well-controlled through the thin composite InGaAs/InAs channel, and by the recessed InP source/drain spacers. This work demonstrates that III-V MOSFETs can scale to the sub-10-nm technology nodes.

**References:**

- [1] ITRS 2013 edition.
- [2] K. H. Goh *et al.*, IEDM 2013, p. 433.
- [3] J. Lin *et al.*, IEDM 2014, p. 574.
- [2] T.-W. Kim *et al.*, IEDM 2013, p. 425.
- [3] S. W. Chang *et al.*, IEDM 2013, p. 417.
- [5] D. H. Kim *et al.*, IEDM 2012, p. 761.
- [6] J. J. Gu *et al.*, IEDM 2012, p. 633.
- [7] M. Radosavljevic *et al.*, IEDM 2009, p. 319.
- [8] S. Lee *et al.*, APL 103, p. 233503 (2013).
- [9] S. Lee *et al.*, VLSI 2014, p. 54.
- [10] C. Y. Huang *et al.*, IEDM 2014, p. 586.



**Fig. 1 (Top)** Device structure of ultrathin body InGaAs/InAs MOSFETs.

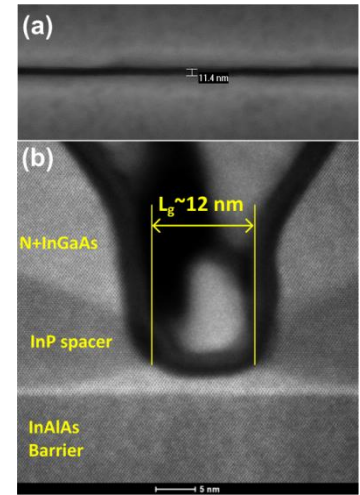


**Fig. 2 (Right)** (a) top-view SEM images before gate metal deposition, showing  $L_g \sim 12$  nm between the edges of regrown layers. (b) TEM image of the final device, showing a  $\sim 2.5$  nm channel, recessed InP source/drain spacers, and  $\sim 12$  nm  $L_g$ .

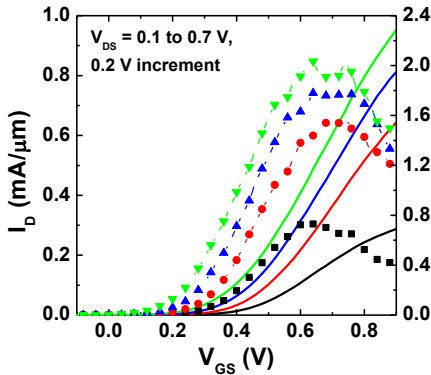


**Fig. 3**  $I_D$  and transconductance  $g_m$  versus  $V_{GS}$  for a 12 nm- $L_g$  FET.

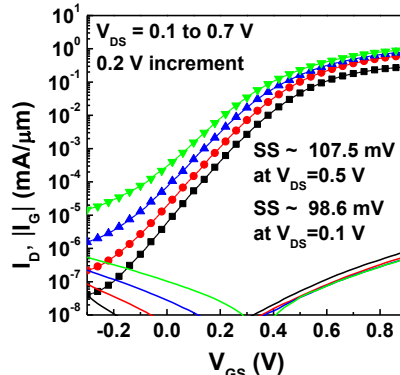


**Fig. 4** Subthreshold characteristics for a 12 nm- $L_g$  FET.

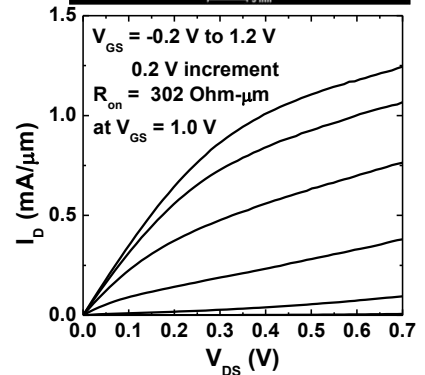


**Fig. 5** Output characteristics for a 12 nm- $L_g$  FET.

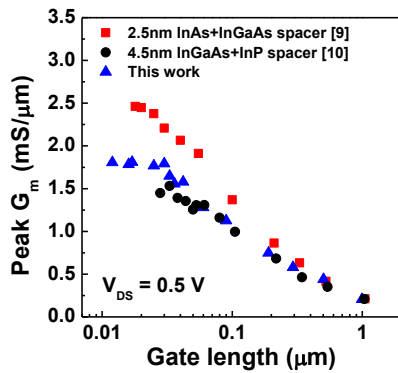


**Fig. 6**  $g_m$  vs.  $L_g$  for this work, compared to [9,10].

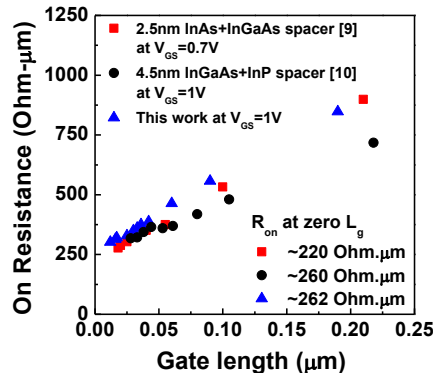


**Fig. 7**  $R_{on}$  vs.  $L_g$  for this work, compared to [9,10].

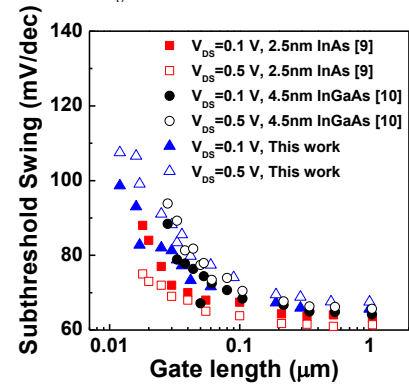


**Fig. 8** SS vs.  $L_g$  for this work, compared to [9,10].

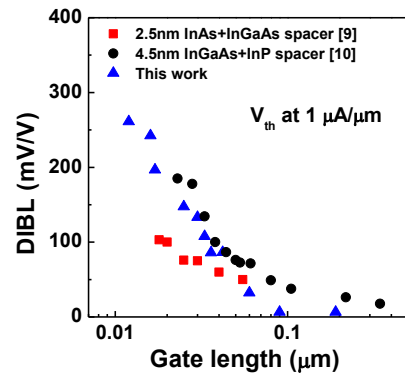


**Fig. 9** DIBL vs.  $L_g$  for this work, compared to [9,10].

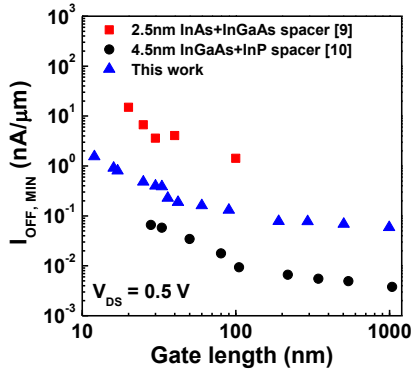


**Fig. 10** Minimum  $I_{off}$  vs.  $L_g$  for this work, compared to [9,10].

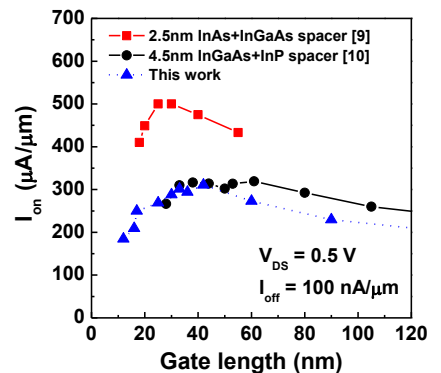


**Fig. 11**  $I_{on}$  vs.  $L_g$  at  $I_{off} = 100$  nA/μm and  $V_{DS} = 0.5$  V.